

Impact and Post-impact Analysis on Engineered Composites



Sunil Chandrakant Joshi and Yi Di Boon

Abstract One of the main downsides of fiber reinforced polymer composite laminates is their susceptibility to impact damage. Many different methods have been devised to either modify or engineer the composites to improve their impact resistance and tolerance. In this chapter, three types of engineered composites and their impact performances are presented and discussed. The engineered composites are (i) composites with core–shell polymer particles, (ii) composites with carbon nanotubes/nanofibers and (iii) composites with thermoplastic film interleaves. Core–shell polymer particles absorb large amounts of energy during impact, thus limit the damage done to the composite laminate. Carbon nanotubes and nanofibers have excellent stiffness and strength, making them suitable for reinforcing the interlaminar regions of composite laminates, leading to improved impact resistance. For composites with thermoplastic film interleaves, thermoplastic films with high intrinsic toughness modify the interlaminar regions of the composite laminate and enhance the overall toughness. The three types of engineered composites exhibit varying levels of improved impact performances compared to the unmodified composites. For each type of engineered composite, its impact response, the strengthening mechanisms and factors affecting its impact performance are deliberated.

Keywords Low velocity impact · Engineered composites · Core shell polymer · Carbon nanotube/nanofiber · Film interleaving

1 Introduction

Fiber reinforced polymer (FRP) composites are popular materials used in structural applications due to their very high specific strengths. One of the main weaknesses of FRP composites is their susceptibility to impact damage, even at low energy levels. Low energy impact coming from tool drops, collision with debris or other events can result in barely visible and difficult-to-detect internal damage to FRP composites,

S. C. Joshi (✉) · Y. Di Boon
School of Mechanical and Aerospace Engineering, Nanyang Technological University, 50,
Nanyang Avenue, Jurong West 639798, Singapore
e-mail: mscjoshi@ntu.edu

© Springer Nature Singapore Pte Ltd. 2021
M. T. H. Sultan et al. (eds.), *Impact Studies of Composite Materials*, Composites Science and Technology, https://doi.org/10.1007/978-981-16-1323-4_7

which affect their load carrying capabilities greatly (Abrate 1991). Therefore, it is important to study the effects of impact and ways to improve impact resistance of FRP composites.

1.1 Impact Damage

Impact events on FRP composite laminates can be categorized as low energy impact, ballistic impact and hypervelocity impact. Ballistic impact is associated with military applications, while hypervelocity impact refers to impact at very high speeds (above 1 km/s) relevant for spacecraft design and analysis (Abrate 1991). For composite materials in structural applications, low energy impact events are more common and will be the focus of the chapter. Low energy or low velocity impact can lead to an internal damage in a laminate, but often produce only a slight indentation to the outer surface of the laminate (termed as barely visible impact damage) (Abrate 1991; Kumar and Rai 1993).

The damage in FRP composites due to impact include fiber breakage, matrix cracking and delamination modes (Abrate 1991; Khan and Kim 2011). For fiber damage modes, impact damage is largely affected by the strain energy absorbing capability of the fiber reinforcement. Fiber reinforcement with high strain to failure leads to composites with improved impact resistance (Cantwell and Morton 1991). The delamination and matrix cracking damage modes are largely dependent on the mechanical properties of the polymer matrix. Many composites in structural applications have brittle matrices (such as epoxy), leading to low resistance to delamination and impact damage (Sela and Ishai 1989).

For low velocity impact, experimental tests that can be performed on FRP composites include the Charpy test, the Izod test and the drop weight impact test. The different test methods have been detailed by Cantwell and Morton (Cantwell and Morton 1991). For the studies discussed in this chapter, the drop weight impact test is used. Figure 1 shows typical load and energy response curves obtained from a drop weight impact test. From the load response curve, damage initiation can be determined by identifying the first load drop occurrence. The load at damage initiation is denoted by L_{init} . The peak load, L_{peak} , can be determined from the highest point of the load response curve. This is the impact load that the composite can withstand before undergoing severe damage (Rahman et al. 2015).

The characteristics determined from the energy response curve are also indicated in Fig. 1. For impact tests without perforation, some energy is transferred back to the impactor, causing the impactor to rebound. This is the elastic portion of the stored energy in the specimen, E_{elas} . The remaining energy, E_{abs} , is absorbed by the specimen, resulting in damage such as delamination (Walker et al. 2002). For impact tests leading to perforation, there is no E_{elas} (impactor does not rebound) and the energy absorbed is also termed the perforation energy. Besides the load and energy response curves, the damage area due to the impact can also be used as a measure

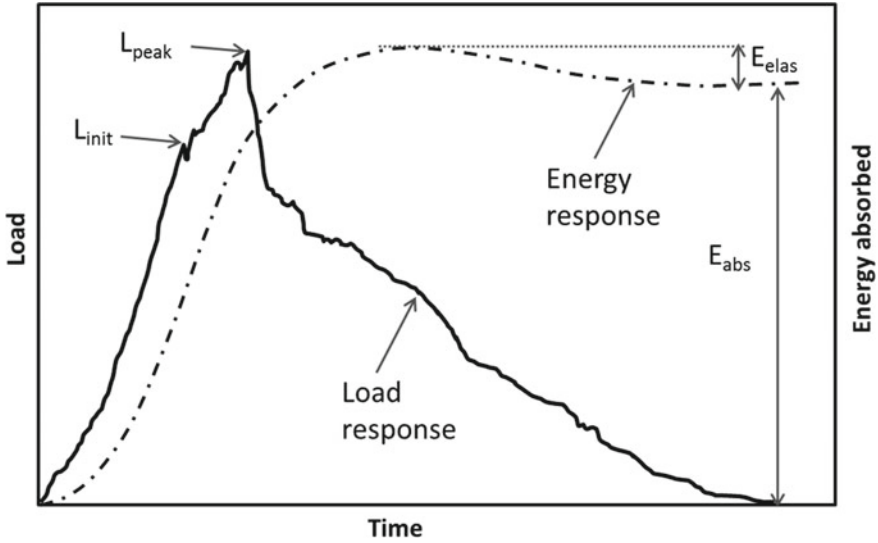


Fig. 1 Typical load and energy vs time responses of FRP composite laminate subjected to low energy impact

of impact resistance. The damage area can be determined using methods such as ultrasonic C-scan.

1.2 Residual Strength

Besides impact resistance, it is also important to study the impact damage tolerance of an FRP composite. Damage tolerance is “the ability of a material to survive a specific amount of damage” (Khan and Kim 2011). Impact damage tolerance can be studied by measuring the residual strength of an FRP composite after being subjected to impact damage.

Compression-after-impact (CAI) tests are used to study the residual compression strength. CAI tests can be performed following the procedure detailed in the ASTM D7137 standard. A fixture to support and guide the test specimen is required to prevent bending and buckling in the specimen during the CAI test. Researchers have also used flexural-after-impact (FAI) tests to study the impact damage tolerance of FRP composites (He et al. 2019; Santiuste et al. 2010). There are currently no specific standards for FAI tests. Three or four point flexural tests (as detailed in standards such as ASTM D790 and D6272) can be carried out on specimens subjected to impact damage to determine the residual flexural strength and stiffness. Strength and stiffness retention factors can be calculated as the ratio of (residual property)/(property of undamaged specimen) (Abrate 1991).

1.3 Engineered Composites

Researchers have studied various methods to engineer or modify FRP composites so that their impact resistance and tolerance can be improved. Some of the methods involve the toughening of the polymer matrix by adding modifiers such as rubber (Bagheri et al. 2009; Yan et al. 2002) and hyper-branched polymers (HPBs) (DeCarli et al. 2005; Verrey et al. 2005). Other methods involve the toughening of the interlaminar regions of FRP composites using short fiber reinforcements made of Kevlar and Zylon (Sohn et al. 2000; Walker et al. 2002). Through thickness reinforcement methods such as z-pinning (Mouritz 2007) and stitching (Tan et al. 2011, 2012) have also been used to improve the impact performance of FRP composites.

In this chapter, three types of engineered composites and their impact responses are addressed. They are (i) composites with core-shell polymer particles, (ii) composites with carbon nanotubes/nanofibers and (iii) composites with thermoplastic film interleaves.

2 Composites with Core-Shell Polymer Particles

In this section, the effects of core-shell polymer (CSH) particles on the impact resistance of FRP composites are discussed. The CSH particles can be used to toughen the interlaminar regions and improve the energy absorption capabilities of FRP composite laminates. The impact responses of composites with CSH particles were studied by Ali and Joshi (Ali 2014; Ali and Joshi 2012, 2013) and Choo (2014).

Figure 2 shows the schematic diagram of a CSH particle. The inner core of the CSH particle is made of poly butyl acrylate (PBA), which is a soft rubber, whereas the rigid outer shell is made of poly (methyl methacrylate) (PMMA), a thermoplastic. Epoxy functional groups are grafted onto the PMMA outer shell so that the CSH particles can bond well with epoxy resin (Ali 2014).

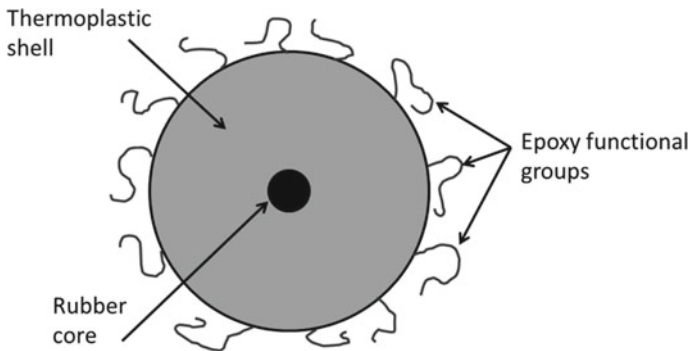


Fig. 2 Structure of the CSH particles

The CSH particles are supplied in white powder form. When observed through a scanning electron microscope (SEM), it can be seen that the CSH particles have varying sizes, ranging from about 20–500 μm . The rubber core has an average size of about 150 nm, while the CSH particle as a whole, including the epoxy functional groups, has an average size of about 160 μm (Ali 2014).

The CSH particles do not agglomerate and are easy to handle compared to other micro- or nano-fillers such as carbon nanotubes (Ali 2014; Ali and Joshi 2012). For the fabrication of FRP composites using the hand layup method, CSH particles can be spread between the FRP prepreg plies before curing. Curing of the FRP composites with CSH particles can be performed in the same manner as composites without CSH particles.

2.1 Impact Response

The impact responses of carbon FRP (CFRP) laminates with and without CSH alteration were investigated by Ali and Joshi (Ali 2014; Ali and Joshi 2012). The test specimens were made using 8 plain weave carbon/epoxy prepregs with fiber volume contents of 60%. For the CSH altered specimens, all of the interlaminar regions (7 in total) were toughened with CSH particles at an areal density of about 50 g/m^2 . Drop weight impact tests were carried out at the energy level of 15 J. The impactor used has a hemispherical shape with 12.7 mm diameter. The average velocity at impact was 3.2 m/s, which is in the velocity range for low velocity impact tests. The test specimens with and without CSH alteration were denoted C-CSH0 and C-CSH50 respectively.

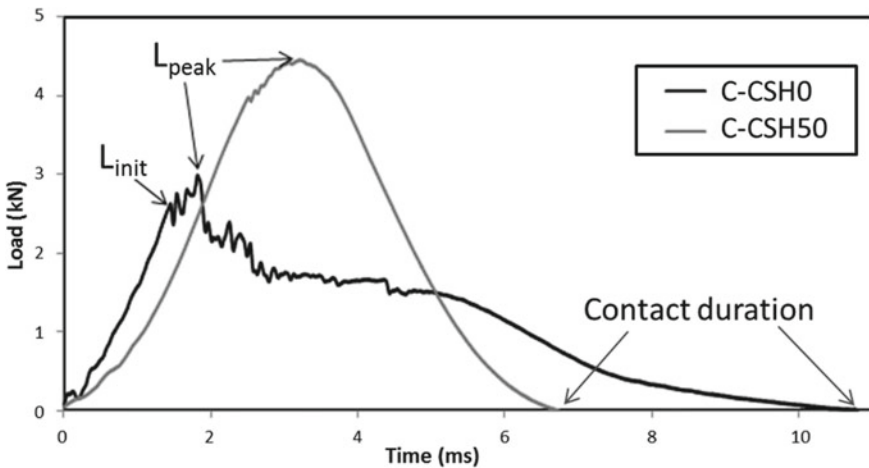


Fig. 3 Impact load responses of C-CSH0 and C-CSH50 laminates

The load-time curves of the impact tests (Ali 2014) are shown in Fig. 3. For both C-CSH0 and C-CSH50 laminates, perforation did not occur. For C-CSH0, damage initiation occurred at the load of 2.52 kN (labeled as L_{init}). After damage initiation, oscillations were recorded in the load-time curve indicating progressive damage taking place in the laminate. The peak load (L_{peak}) occurred at 2.90 kN, followed by a sharp drop in the graph showing that severe damage has occurred (supercritical impact). In contrast, the load-time curve for C-CSH50 has a near symmetrical shape with no significant load drop. This shows that the impact only resulted in minimal damage to the C-CSH50 laminates (subcritical impact). The L_{peak} for C-CSH50 was recorded at 4.09 kN, which is about 41% higher than that of C-CSH0 (Ali 2014; Ali and Joshi 2012).

The extent of damage can also be deduced from the contact duration between the impactor and the test specimens, which can also be determined from Fig. 3. The contact duration for C-CSH0 (average of 10.80 ms) is longer than that of C-CSH50 (average 6.75 ms). The long contact duration for C-CSH0 is due to their larger compliance, which is a consequence of severe impact damage. On the other hand, the C-CSH50 specimens retained high instantaneous stiffness after impact, resulting in short contact duration (Ali 2014; Ali and Joshi 2012).

The energy absorbed during impact for the C-CSH0 and C-CSH50 laminates were also studied (Ali 2014; Ali and Joshi 2012). The addition of CSH particles in the C-CSH50 laminates resulted in an increase of about 230% in E_{elas} and a decrease of about 18% in E_{abs} compared to C-CSH0 laminates. These results show that the CSH particles were very effective in mitigating impact damage in the laminates. The impact test results for the C-CSH0 and C-CSH50 laminates are summarized in Table 1.

Ali and Joshi also studied the performance of CSH altered glass FRP (GFRP) composite laminates subjected to impacts at different energy levels (Ali 2014; Ali and Joshi 2013). Drop weight impact tests (with hemispherical impactor) were carried out at energy levels of about 1.7, 3.3, 4.5, 6.2 and 9.5 J. The test specimens consist of 8 glass/epoxy plies with fiber volume contents of 60% and fibers in the 4-harness satin weave configuration. For the CSH altered specimens (denoted G-CSH30), CSH particles were added to all 7 of the interlaminar regions at the areal density of 30 g/m². Reference unaltered specimens (denoted G-CSH0) were also tested for comparison.

Table 1 Summary of impact test results for C-CSH0 and C-CSH50 laminates (Ali 2014)

Characteristics	C-CSH0	C-CSH50
Damage initiation load, L_{init} (kN)	2.52 (9.3)	–
Peak load, L_{peak} (kN)	2.90 (5.5)	4.09 (8.2)
Contact duration (ms)	10.80 (8.9)	6.75 (7.4)
Elastic energy, E_{elas} (J)	1.06 (9.5)	3.48 (5.8)
Absorbed energy, E_{abs} (J)	12.94 (1.4)	10.68 (1.3)

Note Coefficient of variance given in parenthesis

For the G-CSH0 laminates, subcritical response was observed for impact at energy level 1.7 J while higher impact energies resulted in supercritical impact. On the other hand, for G-CSH30 laminates, subcritical response was recorded for impact at energy levels up to 3.3 J. This shows that the CSH particles improved the GFRP laminate's ability to store energy elastically during impact (similar to results for C-CSH50). At the impact energy of 9.5 J, perforation occurred for both G-CSH0 and G-CSH30 laminates (Ali 2014; Ali and Joshi 2013).

Figure 4 shows the peak loads (L_{peak}) recorded during impact at different energy levels for G-CSH0 and G-CSH30 laminates (Ali and Joshi 2013). At low impact energy (1.7 J), L_{peak} values for G-CSH0 and G-CSH30 are about the same because there was very little damage for both cases (subcritical impact). For higher impact energies, CSH particles improved the impact resistance of the laminates, as shown in the higher L_{peak} for G-CSH30. At impact energy 6.2 J and above, the L_{peak} values became almost constant. This means that the ultimate load bearing capacity has been reached. The ultimate load bearing capacity for G-CSH30 is about 60% higher than that of G-CSH0 (Ali 2014; Ali and Joshi 2013).

Ali and Joshi also conducted four point flexural tests on the G-CSH0 and G-CSH30 laminates to study their flexural performances. The flexural modulus and strength of G-CSH30 were 13% and 19% lower than those of G-CSH0 respectively. The addition of CSH particles had a negative effect on the flexural performance of the GFRP laminate (Ali 2014; Ali and Joshi 2013).

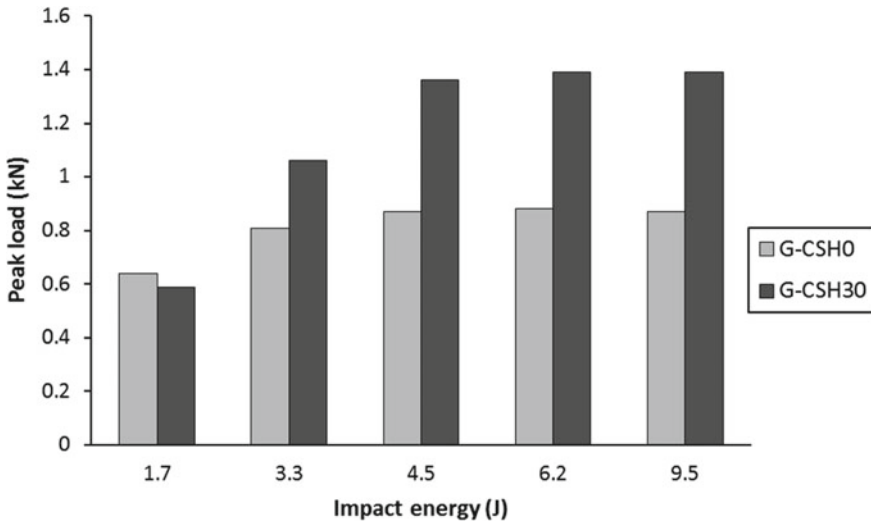


Fig. 4 Peak load versus impact energy for G-CSH0 and G-CSH30 laminates

2.2 Post-impact Analysis

Ali and Joshi studied the interlaminar regions of G-CSH30 laminates after being subjected to impact at 6.2 J using SEM (Ali 2014; Ali and Joshi 2013). The impact energy of 6.2 J resulted in supercritical damage in the G-CSH30 laminates. Figure 5a, b show the cross sections of the damaged laminate taken below the impact point, while Fig. 5c, d show the cross sections at regions away from the impact point. The CSH particles near the point of impact were crushed and broken into smaller pieces. The soft nature of the PMMA shell allows the CSH particles to break under impact load and absorb the impact energy. The broken CSH particles also act to deflect the crack propagation in the epoxy matrix. As a result, cracks in the matrix and delamination are confined to a smaller area of the laminate (Ali 2014; Ali and Joshi 2013). At regions away from the impact point, plastic or tearing deformations in the CSH particles were observed. The tearing deformations consume energy and limit damage to the epoxy matrix due to impact (Ali 2014; Ali and Joshi 2013). These mechanisms combine to improve the impact resistance of the laminate.

Choo conducted CAI tests on GFRP laminates modified with CSH particles to study their impact tolerance (Choo 2014). The laminates studied were made with 8

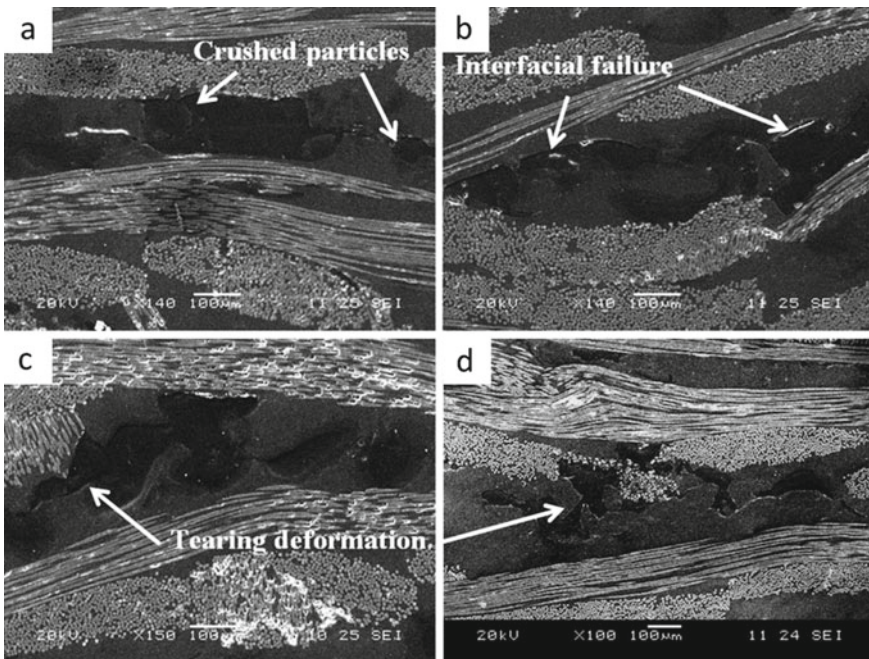


Fig. 5 SEM images of G-CSH30 laminates after supercritical impact: **a** and **b** show cross sectional areas at damaged regions below the point of impact, **c** and **d** show cross sectional areas at regions away from the point of impact (Ali 2014)

layers of glass/epoxy prepregs. CSH particles were added to the interlaminar regions at the areal density of 30 g/m². Reference laminates without CSH particles were also fabricated and tested. The laminates with and without CSH particles are designated G-CSH30-C and G-CSH0-C respectively. Drop weight impact tests were carried out at the energy level of 13.4 J. A hemispherical impactor was used. Compressive tests were carried out following the ASTM D3410 standard using a universal testing machine with wedge grips. Compressive test specimens were cut from the impact test specimens (Choo 2014) as drawn in Fig. 6. The compressive test specimens are labeled 1, 2 and 3 based on their positions relative to the impact point (e.g. G-CSH30-C3 is the compressive test specimen furthest away from the impact point, cut from laminates modified with CSH particles).

The compressive moduli and strengths for G-CSH0 and G-CSH30 before and after impact are presented in Table 2 (Choo 2014). In the undamaged state, G-CSH30 had higher compressive strength (increase of about 15%) but lower compressive modulus (decrease of about 30%) compared to G-CSH0. In order to study the impact tolerance of the laminates, the retention factors for the compressive properties were calculated.

Fig. 6 Compressive test specimens cut from impact test specimens

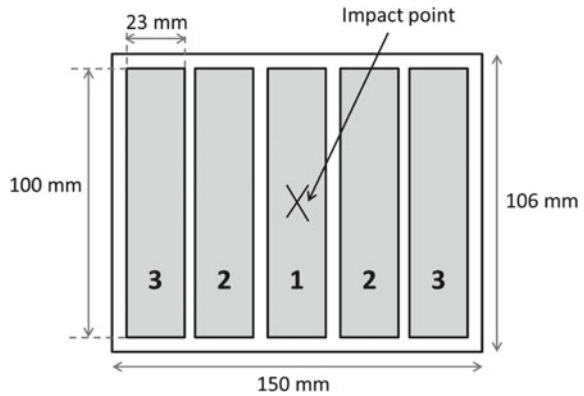


Table 2 Compression-after-impact (CAI) test results for G-CSH0 and G-CSH30 laminates

Specimen	Compressive modulus (MPa)			Compressive strength (MPa)		
	Undamaged (Choo 2014)	Residual (Choo 2014)	Retention factor	Undamaged (Choo 2014)	Residual (Choo 2014)	Retention factor
G-CSH0-C1	710.2	586.3	0.826	207.6	112.8	0.543
G-CSH0-C2	710.2	629.8	0.887	207.6	153.7	0.740
G-CSH0-C3	710.2	667.4	0.940	207.6	208.8	1.01
G-CSH30-C1	494.8	376.9	0.762	239.6	124.1	0.518
G-CSH30-C2	494.8	424.9	0.859	239.6	172.0	0.718
G-CSH30-C3	494.8	464.4	0.939	239.6	239.5	1.00

Note Retention factor = (Residual compressive property)/(Undamaged compressive property)

The retention factors were lower for specimens positioned closer to the point of impact. Overall, the G-CSH30 specimens gave lower retention factors compared to G-CSH0 specimens. This suggests that the CSH particles had a negative effect on the impact damage tolerance of the GFRP laminate.

3 Composites with Carbon Nanotubes/Nanofibers

Carbon-nanotubes (CNTs) and carbon nanofibers (CNFs) are used as nano-fillers for FRP composites because of their high strength and large surface area to volume ratio (Dikshit et al. 2017; Taylor 2010). CNTs and CNFs have been shown to improve the interlaminar fracture toughness of laminated composites (Boon and Joshi 2020; Dikshit et al. 2017; Khan and Kim 2011). Since damage resistance of FRP composites closely relates to the mechanical properties of the interlaminar regions, CNTs and CNFs are also expected to improve the impact performance of FRP composites.

CNTs can be categorized as single walled CNTs (SWCNTs) and multi walled CNTs (MWCNTs) (Taylor 2010). CNTs have a hollow structure and diameters in the order of 1–10 nm. On the other hand, CNFs have a structure made of stacked conical layers and diameters in the order of 100 nm (Kim et al. 2013). CNTs and CNFs can be used in different ways to modify FRP composite laminates, including mixing with the polymer matrix, applied to the interlaminar region (as dry nano-fillers or together with a polymer interleaf), and grafted onto the surface of the fiber reinforcement (Dikshit et al. 2017). One of the main challenges of using CNTs and CNFs is the tendency for the nano-fillers to agglomerate. Without proper dispersion, agglomerated CNTs/CNFs act as defects in FRP composites, leading to negative effects to the mechanical properties of the composites (Taylor 2010).

Researchers have used various methods to disperse and add CNTs/CNFs to FRP composite laminates. One simple method, termed solvent spraying (Fig. 7), is detailed by Dikshit (2014). CNTs are first mixed with ethanol. The mixture is then placed in an ultrasonicator to disperse the CNTs. Subsequently, the mixture is transferred to a sprayer which is used to apply the mixture evenly onto a Teflon sheet. The ethanol solution is allowed to evaporate at elevated temperature, leaving the well dispersed CNTs on the Teflon sheet. The CNTs are then transferred to an FRP composite prepreg by placing the prepreg on top of the Teflon sheet and applying slight pressure using a roller. The prepregs can then be stacked using the hand-layup method and cured to produce composite laminates with CNTs as nano-fillers. The solvent spraying method has been used to achieve good dispersion of CNTs in FRP laminates (Chaudhry et al. 2017; Dikshit 2014; Rodríguez-González et al. 2017). Other methods of dispersing CNTs and CNFs include calendering or the three-roll mill, addition of surfactants, as well as surface functionalization of the nano-fillers (Boon and Joshi 2020).

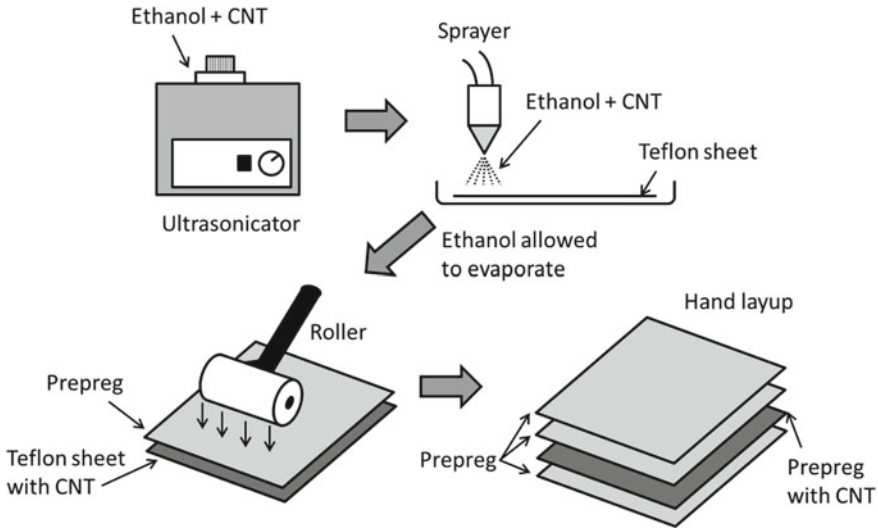


Fig. 7 Schematic of the solvent spraying method

3.1 Impact Response

Kostopoulos et al. studied the impact response of CFRP laminates modified with 0.5 wt.% MWCNT (Kostopoulos et al. 2010). A high shear device was used to disperse the MWCNTs in the epoxy resin. The CFRP laminates have a quasi-isotropic configuration of $[0/+45/90/-45]_{2s}$ and fiber volume fraction of 58%. Reference laminates with neat epoxy matrix were also tested. Drop weight impact tests were conducted at impact energies 2, 8, 12, 16 and 20 J. The impactor used has a hemispherical shape with 20 mm diameter. For all the impact energies tested, the impactor did not penetrate the specimens. From the impact tests, the peak loads and contact durations for the neat and modified specimens were about the same. At low impact energies of 2 and 8 J, there was no difference between the neat and modified specimens in their energy absorbed and delamination area. At higher impact energies of 16 and 20 J, the modified specimens gave slightly higher energy absorption and slightly smaller delamination area compared to the neat specimens. The authors concluded that CNTs can enhance the impact performance of CFRP laminates at higher impact energy levels.

Rahman et al. studied the impact performance of CFRP laminates modified with 1 wt.% oxidized CNFs (Rahman et al. 2015). The sonication process was used to achieve good dispersion of CNFs in the epoxy resin. The test specimens consist of 16 plain woven layers with fiber volume fraction of about 58%. For comparison, test specimens with neat epoxy matrix were also fabricated. Drop weight impact tests were carried out using a testing machine with a hemispherical impactor (12.5 mm diameter) at impact energies of 10, 20 and 30 J. Rahman et al. found that the peak load

during impact for the modified specimens increased by about 11%, 14% and 17% for impact energies of 10, 20 and 30 J respectively compared to the neat specimens. The authors also examined the specimens using ultrasonic C-scan to determine the damage area. The addition of CNFs was found to decrease the damage area due to impact at all three energy levels studied. The largest reduction in damage area (67%) was recorded for the modified specimen subjected to impact at 20 J.

Another study carried out by Taraghi et al. focused on the impact performance of Kevlar/epoxy laminates modified with MWCNT (Taraghi et al. 2014). The MWCNTs were mixed with epoxy resin using a high shear mixer followed by ultrasonication. Woven Kevlar fabrics were used as reinforcements. Laminates with MWCNT contents of 0, 0.3, 0.5 and 1.0 wt.% were prepared by using the hand lay-up technique. Impact testes were carried out at the energy level 45 J using a testing machine with a hemispherical impactor (20 mm diameter). This energy level is higher than the penetration threshold for the unmodified Kevlar/epoxy laminates (30 J). The impact responses of the laminates were studied at room temperature (27 °C) and low temperature (-40 °C) conditions. The impact test results (Taraghi et al. 2014) are plotted in Fig. 8. At room temperature, the specimens with 0.5 wt.% MWCNT gave the highest peak load and absorbed energy, which are about 21% and 35% higher than those of unmodified specimens. However, increasing MWCNT content further resulted in lower peak load and absorbed energy. This is due to agglomeration of MWCNT occurring at high MWCNT content (Taraghi et al. 2014). For low temperature condition, the specimens with 0.3 wt.% MWCNT gave the highest peak load (14% increase) and absorbed energy (35% increase). The epoxy becomes more brittle at lower temperature, thus addition of MWCNT above 0.3 wt.% did not improve the damage resistance further (Taraghi et al. 2014).

3.2 *Post-impact Analysis*

After impact, Rahman et al. examined the fracture surface of the CFRP laminates modified with CNFs using SEM (Rahman et al. 2015). Fiber bridging due to CNFs were observed for the modified CFRP laminate. This results in larger energy being required to propagate the cracks in the matrix. Sword and sheath fracture of the CNFs were also observed. The fracturing of CNFs absorbs the energy from impact and mitigates damage to the CFRP laminate. Many short and curved cracks were also observed, showing that the CNFs worked to deflect the crack growth. Kostopoulos et al. also used SEM to study the effects of CNTs on the impact response of CFRP laminates (Kostopoulos et al. 2010). They reported that CNT pull-out and fracture occurred in the modified laminates, resulting in larger energy absorbed.

Kosopoulos et al. also performed CAI tests and fatigue compression-after-impact (FCAI) tests on the CFRP laminates modified with 0.5 wt.% MWCNT (Kostopoulos et al. 2010). For CAI tests, the procedure detailed in the ASTM D7137 standard was followed. The addition of MWCNT led to an increase of about 15% in CAI modulus, as well as an increase of 12–15% in CAI strength. The authors attributed

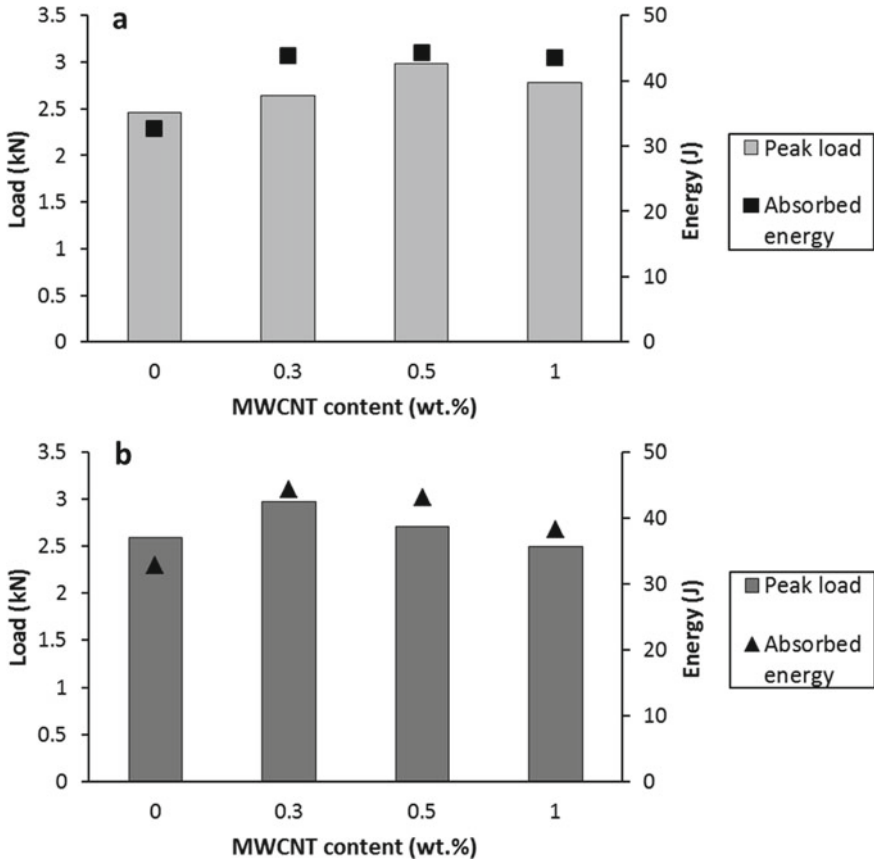


Fig. 8 Impact test (energy level 45 J) results for Kevlar/epoxy laminates with varying MWCNT contents at **a** room temperature (27 °C) and **b** low temperature (-40 °C) conditions

the improved CAI properties to the higher mode I fracture toughness of the MWCNT modified laminates. For the FCAI tests, the MWCNT modified specimens recorded longer fatigue life (by at least 20%) compared to specimens with neat epoxy.

4 Composites with Thermoplastic Film Interleaves

One method to improve the toughness and impact resistance of FRP composites with thermoset matrices is the addition of thermoplastics with high intrinsic toughness. In this section, the toughening of the interlaminar regions in FRP composites using the interleaving method with thermoplastic films is discussed.

Figure 9 shows an FRP laminate toughened using the interleaving method. Researchers have studied the use of many different thermoplastics for interleaving,



Fig. 9 Schematic of FRP laminate with thermoplastic film interleaves

including ethylene vinyl acetate (EVA) (Eldho 2017), polyetherimide (PEI) (Duarte et al. 1999; Gibson et al. 2001), polyetherketone (PEK) (Cheng et al. 2006), polyethylene (PE) (Tanimoto 1994) and poly(ethylene-co-acrylic acid) (PEAA) (Sohn et al. 2000; Walker et al. 2002).

Depending on the interleaf material, the interleaved FRP laminate can be cured in the same way as non-interleaved laminates (co-curing of interleaf with matrix) (Eldho 2017; Sela and Ishai 1989) or with an extra post-curing step (Tanimoto 1994). After curing, the thermoplastic interleaves remain as discrete layers in the laminate (Sela and Ishai 1989). The fabrication process for interleaved laminates remain simple because the properties of the polymer matrix (such as viscosity) remain unchanged during processing (Cheng et al. 2006). The tough thermoplastic interleaves can undergo plastic deformation to absorb energy during impact (Walker et al. 2002). However, the thermoplastic interleaves used for toughening often have low stiffness and strength, leading to lower specific stiffness and strength for the interleaved FRP laminate as well (Sela and Ishai 1989; Walker et al. 2002).

4.1 Impact Response

Duarte et al. studied the impact responses of carbon/epoxy laminates with different types of thermoplastic interleaves (Duarte et al. 1999). The researchers fabricated interleaved CFRP laminates with lay-up $[+45/1/0/I/-45/1/90/1/+45/1/0/I/-45/1/90]_S$ where I refers to the thermoplastic interleaves. The types of interleaves investigated are detailed in Table 3. Non-interleaved CFRP laminates with lay-up $[+45/0/-45/90]_{2S}$ were also fabricated and tested for comparison. Drop weight impact tests were carried out at energy levels of about 1, 2.5, 4 and 6 J/mm. The impactor used was hemispherical with a diameter of 12.5 mm.

Duarte et al. measured the damage area of the impact test specimens using C-scan (Duarte et al. 1999). The specimens with XAF2210 interleaves resulted in smaller damage area compared to the non-interleaved specimens for all impact energy levels studied. In particular, at 6 J/mm, the damage area for XAF2210 specimens was about 55% smaller than that of the non-interleaved specimens. The specimens with the perforated interleaves XAF2210P also resulted in improved impact resistance but the damage area was larger compared to the XAF2210 specimens. On the other hand, the XAF2065 interleaves only gave slight improvement to the impact resistance

Table 3 Thermoplastic interleaves studied by Duarte et al. (1999)

Designation	Material	Molded thickness (mm)	Melting temperature (°C)	Interleaf structure
1a8s18	Copolyamide	0.018	145	Web-like structure
XAF2210	Polyolefin	0.030	145	Thin film
XAF2210P	Polyolefin	0.030	145	Perforated XAF2210, hole size 0.25 in, at 20 mm staggered spacing
XAF2065	Polyolefin	0.039	125	Open net form of XAF2210
ULTEM 1000	Polyetherimide	0.048	225	Thin Film

of the CFRP laminates. For instance, at impact energy of 6 J/mm, the XAF2065 specimens resulted in only about 15% smaller damage area compared to that of the non-interleaved specimens. Therefore, among the specimens with polyolefin interleaves, the specimens with the film type interleaves (XAF2210) showed the best impact resistance.

For the specimens with 1a8s18 interleaves, Duarte et al. reported that the damage area was larger than that of the non-interleaved specimens (Duarte et al. 1999). This was attributed to the web-like structure of the 1a8s18 interleaves and the poor bonding between the copolyamide and the epoxy matrix. The poor bonding resulted in the 1a8s18 interleaves acting as weak points in the laminate for crack initiation. On the other hand, improved impact resistance was achieved with the polyetherimide interleaves (ULTEM 1000). Impact damage was observed on the specimens with ULTEM 1000 interleaves starting at the impact energy of 2.7 J/mm. For impact energies between 2.7 and 5 J/mm, the damage area for the specimens with ULTEM 1000 interleaves was smaller than that of non-interleaved specimens. However, for impact energies above 5 J/mm, the impact resistance of the laminates was not affected by the ULTEM 1000 interleaves. The authors explained that this is due to fiber breakage being the main damage mode for laminates subjected to impact at high energies (Duarte et al. 1999).

Another study on the impact response of CFRP laminates toughened with thermoplastic interleaves was performed by Cheng et al. (2006). The composite laminates studied were made of carbon fiber as reinforcement and bismaleimide (BMI) resin as matrix. Polyetherketone with a phenolphthalein side group (denoted PEK-C) was used as the toughening agent. Cheng et al. studied 4 types of CFRP laminates where the matrix components were toughened with different methods. The 4 types of specimens are (i) specimens with neat BMI as matrix (control case), (ii) specimens with BMI/PEK-C blend as matrix (termed in-situ toughening), (iii) specimens with BMI matrix and PEK-C film interleaves, and (iv) specimens with BMI matrix and BMI/PEK-C blend film interleaves. For the PEK-C toughened specimens, the PEK-C content in the specimens was set to 17.5 wt.%. The specimens were subjected to

Table 4 Impact experiment results of carbon/BMI laminates with different thermoplastic toughening methods studied by Cheng et al. 2006

Case	Composition of matrix	Damage area (mm ²) Cheng et al. (2006)
TP0	BMI matrix (control case)	544
TP1	BMI/PEK-C blend as matrix, PEK-C content at 17.5 wt.%	408
TP2	BMI matrix with PEK-C film interleaves, overall PEK-C content at 17.5 wt.%	345
TP3	BMI matrix with BMI/PEK-C blend film interleaves, overall PEK-C content at 17.5 wt.%	220

impact at impact energy 2 J/mm. The delamination area due to impact was determined using ultrasonic C-scan. The impact test results are summarized in Table 4. Specimens toughened by film interleaving were found to perform better than specimens with in-situ toughening. For film interleaving, the BMI/PEK-C blend film was reported to give smaller impact damage area than the PEK-C film.

4.2 Post-impact Analysis

Duarte et al. studied the undamaged compression strengths and CAI strengths of the CFRP laminates with different thermoplastic interleaves (Table 3) (Duarte et al. 1999). For specimens with XAF2210 interleaves, the undamaged compression strength was 65% lower than that of non-interleaved specimens. Further investigation using a microscope revealed that fiber micro buckling occurred in the specimens leading to the low compression strength. This was due to the low shear modulus of the polyolefin interleaf. The CAI performance of the specimens with XAF2210 interleaves was also worse than non-interleaved specimens. Therefore, although the XAF2210 interleaves reduced the impact damage area, their low shear modulus resulted in significant reduction to the compression strength of the CFRP laminate.

In contrast, CFRP laminates with ULTEM 1000 interleaves had higher undamaged compression strength compared to non-interleaved laminates. This is because of the high shear modulus of polyetherimide (Duarte et al. 1999). Microscopic studies of the ULTEM 1000 interleaved specimens after impact revealed that cracks tend to propagate in the transverse direction through the lamina but not along the interlaminar regions. The ULTEM 1000 interleaves resulted in higher interlaminar fracture toughness for the interleaved specimens. For CAI tests, at impact energy of 1 J/mm, the ULTEM 1000 interleaved specimens gave very high residual strength (93% of undamaged strength) compared to non-interleaved specimens (70% of undamaged strength). However, the improvement in CAI strength became less significant at higher impact energy levels. For instance, ULTEM 1000 interleaved specimens gave 53% residual strength after 4.1 J/mm impact whereas non-interleaved specimens resulted in 40% residual strength after 4.3 J/mm impact (Duarte et al. 1999).

Table 5 Compression-after-impact (CAI) test results for carbon/BMI laminates toughened with PEK-C

Case	Composition of matrix	CAI strength (MPa) Cheng et al. (2006)
TP0	BMI (control case)	180
TP1	BMI/PEK-C blend, PEK-C content at 17.5 wt.%	199
TP2	BMI matrix with PEK-C film interleaves, overall PEK-C content at 17.5 wt.%	254
TP3-a	BMI matrix with BMI/PEK-C blend film interleaves, interleaf weight ratio of BMI:PEK-C = 10:90	256
TP3-b	BMI matrix with BMI/PEK-C blend film interleaves, interleaf weight ratio of BMI:PEK-C = 20:80	272
TP3-c	BMI matrix with BMI/PEK-C blend film interleaves, interleaf weight ratio of BMI:PEK-C = 40:60, overall PEK-C content at 17.5 wt.%	290

Cheng et al. also studied the impact tolerance of carbon/BMI laminates toughened with PEK-C using CAI tests with impact energy 2 J/mm (Cheng et al. 2006). The CAI test results are summarized in Table 5. For specimens toughened with BMI/PEK-C blend film (cases TP3-a, TP3-b and TP3-c in Table 5), the researchers studied three different blend compositions for the film interleaves. The specimens with BMI/PEK-C blend film interleaves at weight ratio of BMI: PEK-C = 40:60 (case TP3-c) gave the highest CAI strength of 290 MPa. The morphology of the interlaminar regions for the carbon/BMI laminates toughened with BMI/PEK-C blend film interleaves was studied using SEM. The researchers reported a fine granular morphology (average diameter of 1 μm) at the interlaminar regions of the laminates (Cheng et al. 2006). The granular morphology was not present for the laminates toughened using PEK-C film interleaves (case TP2). This suggests that the morphology at the interlaminar regions of composite laminates is important in determining their impact resistance and tolerance.

5 Conclusions

CSH particles have been shown to be effective in improving the impact resistance of FRP composite laminates. In particular, laminates modified with the particles showed improved elastic energy storing capabilities during impact. The soft outer shell of the CSH particles generally gets crushed during impact, absorbing energy in the process. Other strengthening mechanisms due to the particles include crack deflection and plastic deformation. These mechanisms combine to hinder crack propagation and limit the severity of impact damage sustained by the modified laminates. However, impact damage tolerance is not improved by the addition of CSH particles.

Researchers have modified FRP composites using CNTs/CNFs and achieved varying levels of improvement to the impact resistance and tolerance of the composites. Fiber bridging and pull-out due to the nano-fillers absorb large amounts of energy, thus reducing the energy available for damage creation in the modified laminates. The nano-fillers also work to hinder crack propagation through crack deflection. Studies have shown that CNTs/CNFs are effective at improving the impact resistance of FRP composite laminates subjected to impact at high energy levels.

The interleaving method is a simple way to toughen the interlaminar regions of FRP composites. For interleaving with thermoplastic films, the improvement to the impact performance of the FRP composite is affected by various factors, including the mechanical properties of the thermoplastic and the resulting morphology of the interlaminar regions. Besides having high toughness, the thermoplastic also needs to have high shear modulus for the thermoplastic film interleave to be effective in toughening the composites.

Comparing the three types of engineered composites, the composites with CSH particles and composites with thermoplastic film interleaves are preferred when ease of manufacturing is important. However, CSH particles and thermoplastic film interleaves both result in reduced in-plane mechanical properties in the composite. This reduction needs to be compensated for with thicker or larger structures, leading to increased weight. For composites with CNTs/CNFs, further studies need to be carried out to optimize their impact performances. In particular, the dispersion process of nano-fillers needs to be further improved to enable higher nano-filler content in the modified composite laminate.

References

- Abrate S (1991) Impact on laminated composite materials. *Appl Mech Rev* 44:155–190. <https://doi.org/10.1115/1.3119500>
- Ali M (2014) Impact behaviour of prepreg laminates with dispersed core/shell particles in ply interfaces. Nanyang Technological University, Singapore
- Ali M, Joshi SC (2012) Impact damage resistance of CFRP prepreg laminates with dispersed CSP particles into ply interfaces. *Int J Damage Mech* 21:1106–1127. <https://doi.org/10.1177/1056789511429143>
- Ali M, Joshi SC (2013) Damage evolution in glass/epoxy composites engineered using core–shell microparticles under impact loading *Journal of Materials Science* 48:8354–8367 doi:<https://doi.org/10.1007/s10853-013-7635-8>
- Bagheri R, Marouf BT, Pearson RA (2009) Rubber-toughened epoxies: a critical review. *Polym Rev* 49:201–225. <https://doi.org/10.1080/15583720903048227>
- Boon YD, Joshi SC (2020) A review of methods for improving interlaminar interfaces and fracture toughness of laminated composites *Materials Today. Communications* 22:100830. <https://doi.org/10.1016/j.mtcomm.2019.100830>
- Cantwell WJ, Morton J (1991) The impact resistance of composite materials — a review *Composites* 22:347–362 doi:[https://doi.org/https://doi.org/10.1016/0010-4361\(91\)90549-V](https://doi.org/https://doi.org/10.1016/0010-4361(91)90549-V)
- Chaudhry MS, Czekanski A, Zhu ZH (2017) Characterization of carbon nanotube enhanced interlaminar fracture toughness of woven carbon fiber reinforced polymer composites. *Int J Mech Sci* 131–132:480–489. <https://doi.org/10.1016/j.ijmecsci.2017.06.016>

- Cheng Q, Fang Z, Xu Y, Yi X-S (2006) Improvement of the Impact Damage Resistance of BMI/Graphite Laminates by the Ex-situ Method. *High Perform Polym* 18:907–917. <https://doi.org/10.1177/0954008306068296>
- Choo KCJ (2014) Compression after impact studies on composite laminates. Nanyang Technological University, Singapore
- DeCarli M, Kozielski K, Tian W, Varley R (2005) Toughening of a carbon fibre reinforced epoxy anhydride composite using an epoxy terminated hyperbranched modifier. *Compos Sci Technol* 65:2156–2166. <https://doi.org/10.1016/j.compscitech.2005.05.003>
- Dikshit V (2014) Manufacturing and performance studies of laminated composites with nano-reinforced inter-ply interfaces. Nanyang Technological University, Singapore
- Dikshit V, Bhudolia S, Joshi S (2017) Multiscale Polymer Composites: A Review of the Interlaminar Fracture Toughness Improvement *Fibers* 5:38
- Duarte A, Herszberg I, Paton R (1999) Impact resistance and tolerance of interleaved tape laminates. *Compos Struct* 47:753–758. [https://doi.org/10.1016/S0263-8223\(00\)00049-0](https://doi.org/10.1016/S0263-8223(00)00049-0)
- Eldho M (2017) Effects of thermoplastic film interleaving on fracture toughness of GFRP laminates. Nanyang Technological University, Singapore
- Gibson RF, Chen Y, Zhao H (2001) Improvement of Vibration Damping Capacity and Fracture Toughness in Composite Laminates by the Use of Polymeric Interleaves. *J Eng Mater Technol* 123:309–314. <https://doi.org/10.1115/1.1370385>
- He W, Lu S, Yi K, Wang S, Sun G, Hu Z (2019) Residual flexural properties of CFRP sandwich structures with aluminum honeycomb cores after low-velocity impact. *Int J Mech Sci* 161–162:105026. <https://doi.org/10.1016/j.ijmecsci.2019.105026>
- Khan SU, Kim J-K (2011) Impact and delamination failure of multiscale carbon nanotube-fiber reinforced polymer composites: a review *International Journal of Aeronautical and Space Science* 12:115–133. <https://doi.org/10.5139/IJASS.2011.12.2.115>
- Kim YA, Hayashi T, Endo M, Dresselhaus MS (2013) Carbon nanofibers. In: Vajtai R (ed) *Springer Handbook of Nanomaterials*. Springer, Berlin, Heidelberg, pp 233–262
- Kostopoulos V, Baltopoulos A, Karapappas P, Vavouliotis A, Paipetis A (2010) Impact and after-impact properties of carbon fibre reinforced composites enhanced with multi-wall carbon nanotubes. *Compos Sci Technol* 70:553–563. <https://doi.org/10.1016/j.compscitech.2009.11.023>
- Kumar P, Rai B (1993) Delaminations of barely visible impact damage in CFRP laminates. *Compos Struct* 23:313–318. [https://doi.org/10.1016/0263-8223\(93\)90231-E](https://doi.org/10.1016/0263-8223(93)90231-E)
- Mouritz AP (2007) Review of z-pinned composite laminates. *Compos A Appl Sci Manuf* 38:2383–2397. <https://doi.org/10.1016/j.compositesa.2007.08.016>
- Rahman MM, Hosur M, Hsiao K-T, Wallace L, Jeelani S (2015) Low velocity impact properties of carbon nanofibers integrated carbon fiber/epoxy hybrid composites manufactured by OOA–VBO process *Composite Structures* 120:32–40. <https://doi.org/10.1016/j.compstruct.2014.09.053>
- Rodríguez-González JA, Rubio-González C, Meneses-Nochebuena CA, González-García P, Licea-Jiménez L (2017) Enhanced interlaminar fracture toughness of unidirectional carbon fiber/epoxy composites modified with sprayed multi-walled carbon nanotubes. *Compos Interfaces* 24:883–896. <https://doi.org/10.1080/09276440.2017.1302279>
- Santiuste C, Sanchez-Saez S, Barbero E (2010) Residual flexural strength after low-velocity impact in glass/polyester composite beams. *Compos Struct* 92:25–30. <https://doi.org/10.1016/j.compstruct.2009.06.007>
- Sela N, Ishai O (1989) Interlaminar fracture toughness and toughening of laminated composite materials: a review. *Composites* 20:423–435. [https://doi.org/10.1016/0010-4361\(89\)90211-5](https://doi.org/10.1016/0010-4361(89)90211-5)
- Sohn MS, Hu XZ, Kim JK, Walker L (2000) Impact damage characterisation of carbon fibre/epoxy composites with multi-layer reinforcement. *Compos B Eng* 31:681–691. [https://doi.org/10.1016/S1359-8368\(00\)00028-7](https://doi.org/10.1016/S1359-8368(00)00028-7)
- Tan KT, Watanabe N, Iwahori Y (2011) Impact damage resistance, response, and mechanisms of laminated composites reinforced by through-thickness stitching. *Int J Damage Mech* 21:51–80. <https://doi.org/10.1177/1056789510397070>

- Tan KT, Watanabe N, Iwahori Y, Ishikawa T (2012) Understanding effectiveness of stitching in suppression of impact damage: an empirical delamination reduction trend for stitched composites. *Compos A Appl Sci Manuf* 43:823–832. <https://doi.org/10.1016/j.compositesa.2011.12.022>
- Tanimoto T (1994) Suppression of interlaminar damage in carbon/epoxy laminates by use of interleaf layers. *Scr Metall Mater* 31:1073–1078. [https://doi.org/10.1016/0956-716X\(94\)90529-0](https://doi.org/10.1016/0956-716X(94)90529-0)
- Taraghi I, Fereidoon A, Taheri-Behrooz F (2014) Low-velocity impact response of woven Kevlar/epoxy laminated composites reinforced with multi-walled carbon nanotubes at ambient and low temperatures. *Mater Des* 53:152–158. <https://doi.org/10.1016/j.matdes.2013.06.051>
- Taylor AC (2010) Advances in nanoparticle reinforcement in structural adhesives. In: Dillard DA (ed) *Advances in structural adhesive bonding*. Woodhead Publishing Limited, Cambridge, UK, pp 151–182
- Verrey J, Winkler Y, Michaud V, Manson JAE (2005) Interlaminar fracture toughness improvement in composites with hyperbranched polymer modified resin. *Compos Sci Technol* 65:1527–1536. <https://doi.org/10.1016/j.compscitech.2005.01.005>
- Walker L, Sohn M-S, Hu X-Z (2002) Improving impact resistance of carbon-fibre composites through interlaminar reinforcement. *Compos A Appl Sci Manuf* 33:893–902. [https://doi.org/10.1016/S1359-835X\(02\)00010-6](https://doi.org/10.1016/S1359-835X(02)00010-6)
- Yan C, Xiao K, Ye L, Mai Y-W (2002) Numerical and experimental studies on the fracture behavior of rubber-toughened epoxy in bulk specimen and laminated composites. *J Mater Sci* 37:921–927. <https://doi.org/10.1023/A:1014335511515>